ACS OMEGA

http://pubs.acs.org/journal/acsodf

Article

Thermodynamic and Kinetic Studies on Adsorption of Vanadium with Glutamic Acid

Hao Peng,* Hongzhi Qiu, Caiqiong Wang, Binfang Yuan, Huisheng Huang, and Bing Li*

Cite This: *ACS Omega* 2021, 6, 21563−21570

Read Online

ACCESS | Metrics & More | Article Recommendations

ABSTRACT: Many hydrometallurgy methods, including chemical precipitation, ion exchange, solvent extraction, and adsorption, have been used to recover vanadium from vanadium solution, but the final step of these methods involved precipitation with ammonium salts, high concentrations of which are harmful to the environment. The key point is to find a new compound to replace ammonium salts without reducing the vanadium precipitation efficiency. The adsorption process of vanadium with glutamic acid is investigated. The effects of experimental factors, including dosage of glutamic acid, reaction temperature, concentration of H_2SO_4, and reaction time, on the adsorption process are investigated. The results show that nearly 91.66% vanadium is adsorbed under the following reaction conditions: reaction temperature of 90 °C, H_2SO_4 concentration of 20 g/L, glutamic acid dosage at $n(glu)/n(V)$ = 3.0:1, and reaction time of 60 min. The response surface methodology is applied to optimize the reaction conditions. The analysis results indicate that the reaction temperature has the greatest effect on the adsorption efficiency of vanadium and the influence of experimental factors follows the order: reaction temperature > dosage of glutamic acid to vanadium > reaction time > concentration of H_2SO_4. The pseudo-second-order model is selected to describe well the adsorption kinetic behavior, and the thermodynamic analysis results indicate that the adsorption process of vanadium is unspontaneous and exothermic. The results will be useful for further applications of glutamic acid, and they provide a bright future for vanadium recovery.

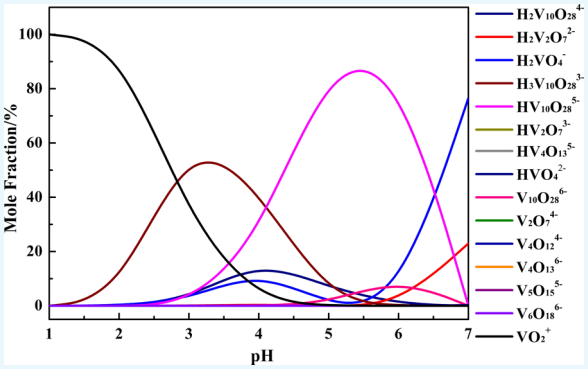

1. INTRODUCTION

Vanadium is widely used in the petrochemical industry, catalysts, and iron steel, due to the excellent physicochemical properties, and it is called "the vitamin of modern industry".[1−6] It is mainly leached out from titanium magnetite and stone coal by hydrometallurgy technologies[7−15] and recovered by technologies like chemical precipitation,[16−20] ion exchange,[21,22] solvent extraction,[10,23−26] and adsorption.[27−31] Among them, chemical precipitation with ammonium salts is the most common method, and vanadium is precipitated in the form of $(NH_4)_2V_6O_{16}$. The whole vanadium recovery efficiency can be up to 95%. However, the large amount of ammonium wastewater is still a problem.[17,32−34]

In recent years, many methods have been developed to achieve high vanadium recovery efficiency. The key point is to find a new compound to replace ammonium salts without reducing the vanadium precipitation efficiency. Adsorption technology has been proven to be an efficient and economical technique because of high efficiency, low input, and simple operation.[35−37] In our previous studies,[27,28,38] melamine exhibited nearly 100% vanadium adsorption efficiency due to the functional group $-NH_2$; thus, kinds of amino acid have attracted our attention.

Glutamic acid (GA) is a white powder widely used in food additives, medicine, feed, industry, and reagents. In this paper, GA is used as an adsorbent to adsorb vanadium. The effects of experimental factors, including dosage of GA, concentration of H_2SO_4, reaction temperature, and reaction time, on the adsorption process are investigated. Meanwhile, the reaction conditions are optimized with response surface methodology.[39−42] Also, the adsorption kinetic behavior and thermodynamic analyses are performed.

2. RESULTS AND DISCUSSION

2.1. The Composition in the Solution. A mole fraction distribution diagram of V(V)-species in a V-H_2O system is obtained at pH = 1−7 and [V] = 0.05 mol/L at 25 °C, and the results are shown in Figure 1.[6] It can be seen that the V(V)

Received: May 18, 2021
Accepted: July 29, 2021
Published: August 11, 2021

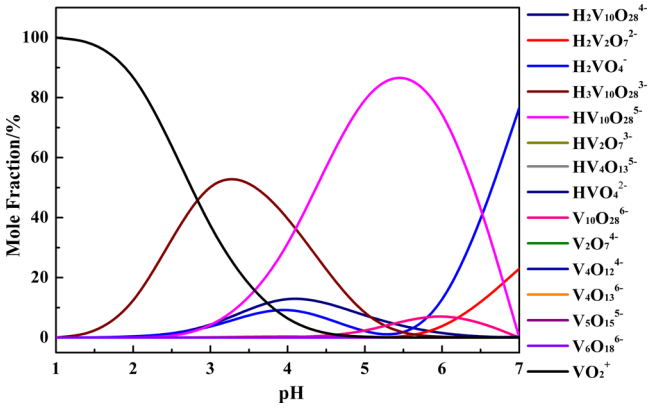

Figure 1. V-species in the V-H_2O system at 25 °C with [V] = 0.05 mol/L.

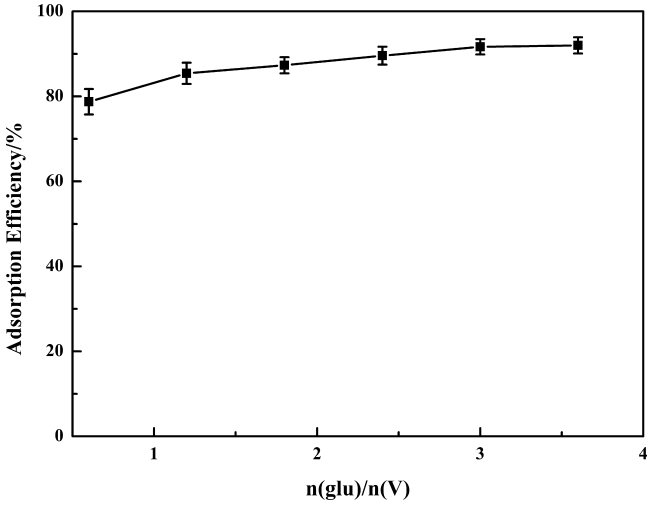

Figure 2. Effect of dosage of glutamic acid on the adsorption efficiency of vanadium.

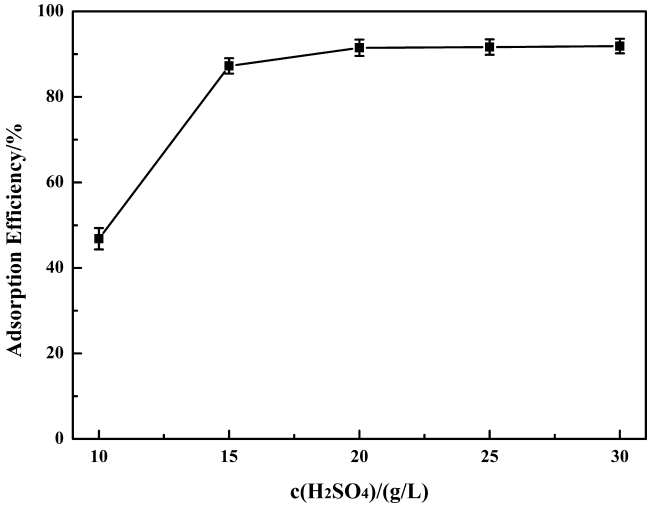

Figure 3. Effect of the concentration of H_2SO_4 on the adsorption efficiency of vanadium.

exists in the form of VO_2^+, HVO_4^{2-}, $H_2VO_4^-$, $V_2O_7^{4-}$, $HV_2O_7^{3-}$, $H_2V_2O_7^{2-}$, $V_4O_{12}^{4-}$, $V_4O_{13}^{6-}$, $HV_4O_{13}^{5-}$, $V_5O_{15}^{5-}$, $V_6O_{18}^{6-}$, $V_{10}O_{28}^{6-}$, $HV_{10}O_{28}^{5-}$, $H_2V_{10}O_{28}^{4-}$, and $H_3V_{10}O_{28}^{3-}$. At the pH range of 1−7, the main species of V(V) in the

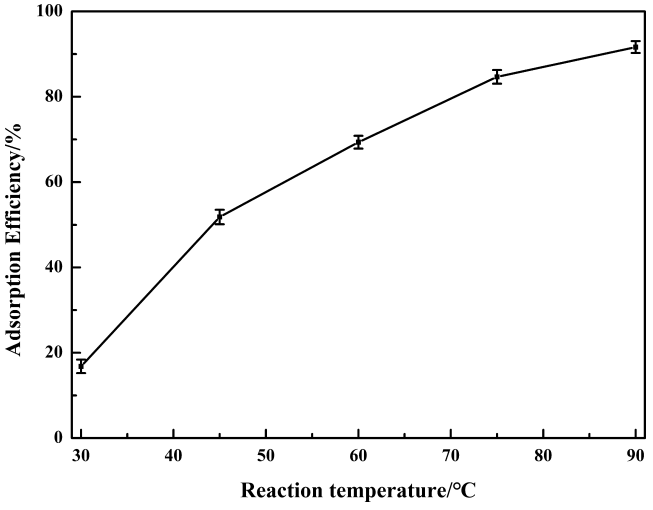

Figure 4. Effect of reaction temperature on the adsorption efficiency of vanadium.

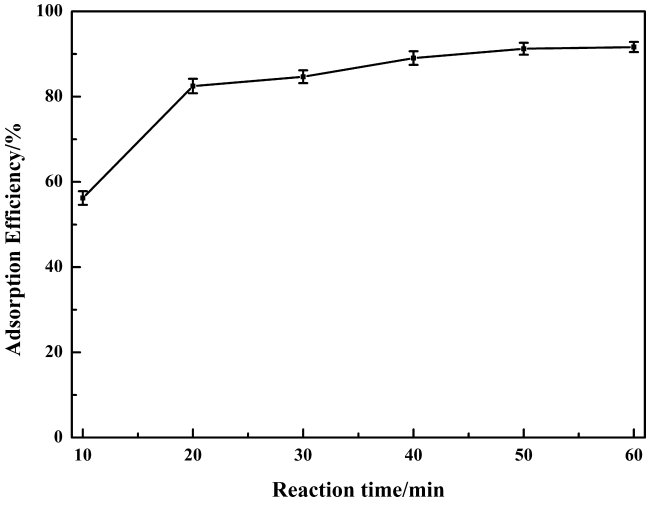

Figure 5. Effect of reaction time on the adsorption efficiency of vanadium.

Table 1. Independent Variables and Factor Levels

independent variable	unit	level		
		−1	0	1
A: concentration of H_2SO_4	g/L	0.00	15.00	30.00
B: reaction temperature	°C	30.00	60.00	90.00
C: reaction time	min	10.00	35.00	60.00
D: n(glu)/n(V)		0.00	1.50	3.00

solution areVO_2^+, $H_3V_{10}O_{28}^{3-}$, and $HV_{10}O_{28}^{5-}$. Almost 100% of V(V) in the solution exists in the form of VO_2^+ when pH = 1. As the pH value increases, the mole fraction of VO_2^+ decreases gradually and VO_2^+ starts to transform into $H_3V_{10}O_{28}^{3-}$, and the mole fraction of $H_3V_{10}O_{28}^{3-}$ reaches 63.8% at pH = 3. On further increasing the pH, $H_3V_{10}O_{28}^{3-}$ gradually transforms into $HV_{10}O_{28}^{5-}$, with the corresponding mole fraction reaching the max value of 86.5% at pH = 5.5.

2.2. Single-Factor Experiments. *2.2.1. Effect of Dosage of GA.* The dosage of GA has a significant effect on the adsorption efficiency, which plays the role of a reaction reagent. A series of experiments is conducted to investigate the effect of n(glu)/n(V) on the adsorption efficiency. The dosage

https://doi.org/10.1021/acsomega.1c02590
ACS Omega 2021, 6, 21563−21570

Table 2. CCD Experimental Matrix and Experimental Results for This Study

run	n(glu)/n(V)	concentration of H_2SO_4	reaction time/min	reaction temperature/°C	adsorption efficiency/%
1	1.5	10	35	30	3.61
2	1.5	20	10	30	63.88
3	1.5	20	60	30	5.42
4	3.0	20	35	30	10.90
5	0.0	20	35	30	4.55
6	1.5	30	35	30	5.29
7	0.0	10	35	60	27.05
8	1.5	10	10	60	73.40
9	1.5	10	60	60	35.57
10	3.0	10	35	60	66.59
11	1.5	20	35	60	22.70
12	3.0	20	60	60	42.73
13	3.0	20	10	60	27.14
14	1.5	20	35	60	36.75
15	1.5	20	35	60	36.75
16	0.0	20	10	60	20.31
17	1.5	20	35	60	36.75
18	0.0	20	60	60	9.36
19	1.5	20	35	60	36.75
20	1.5	30	60	60	5.42
21	1.5	30	10	60	13.48
22	0.0	30	35	60	6.30
23	3.0	30	35	60	7.17
24	1.5	10	35	90	90.72
25	1.5	20	60	90	76.79
26	0.0	20	35	90	61.82
27	3.0	20	35	90	81.61
28	1.5	20	10	90	70.12
29	1.5	30	35	90	57.44

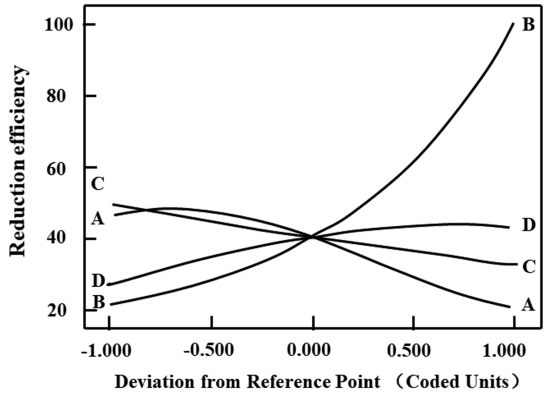

Figure 6. Perturbation plot for the adsorption efficiency of vanadium in the design space. Concentration of H_2SO_4 (A), reaction temperature (B), reaction time (C), and dosage of glutamic acid to vanadium (n(glu)/n(V)) (D).

of GA is set as n(glu)/n(V) = 0.6, 1.2, 1.8, 2.4, 3.0, and 3.6, respectively. In addition, the other reaction conditions are as follows: a reaction time of 60 min, reaction temperature of 90 °C, and H_2SO_4 concentration of 20 g/L. The results shown in Figure 2 indicate that the dosage of GA has a significant effect on the adsorption process and the adsorption efficiency of vanadium increases with the increasing n(glu)/n(V) value. During the adsorption process, the VO_2^+ was adsorbed on the surface of GA by hydrogen bonds or van der Waals force. There are not enough vacant sites for vanadium adsorption on the GA surface at low GA dosage, and the number of vacant sites increases with the increase of GA dosage.[43] Thus, the adsorption efficiency increases with a continuous increase of GA dosage. The adsorption efficiency of vanadium increased from 74.48 to 91.66% as dosage of GA increased from n(glu)/n(V) = 0.6 to n(glu)/n(V) = 3.0. A further increase of GA had no obvious effect on adsorption efficiency; thus, n(glu)/n(V) = 3.0 is selected as an optimal condition for further experiments. Though the adsorption efficiency is not as good as that of melamine, which has three $-NH_2$, while GA has only one $-NH_2$,[27,28] the vanadium can still be recovered efficiently.

2.2.2. Effect of the Concentration of H_2SO_4. The existence of vanadium ions has a significant effect on the vanadium recovery process. A series of experiments is conducted to investigate the effect of the concentration of H_2SO_4 on the adsorption efficiency of vanadium, which is set as 10, 15, 20, 25, and 30 g/L, while other reaction conditions are kept constant: n(glu)/n(V) = 3.0, a reaction time of 60 min, and a reaction temperature of 90 °C. Figure 3 shows that the adsorption efficiency of vanadium increases with the increasing concentration of H_2SO_4. Only 46.85% vanadium is adsorbed at a concentration of 10 g/L as vanadium exists as polyanions, which is not beneficial for adsorption.[28] Increasing the concentration of H_2SO_4 can make the solution acidic, and vanadium will transform into cations. When the concentration of H_2SO_4 is over 20 g/L (pH < 1.5), vanadium mostly exists as VO_2^+, which makes a great contribution to high adsorption efficiency of vanadium.[38,43,44] Further increasing the concentration has no obvious effect on adsorption efficiency; thus, 20 g/L is chosen as the optimal concentration of H_2SO_4 for further experiments.

https://doi.org/10.1021/acsomega.1c02590
ACS Omega 2021, 6, 21563−21570

Table 3. Analysis of Variance (ANOVA) for the Response

source	sum of squares	*Df*	mean square	*F* value	*p*-value Prob > *F*
model	26.56	14	1.90	5.19	0.0020
A	5.66	1	5.66	15.47	0.0015
B	14.03	1	14.03	38.38	<0.0001
C	0.97	1	0.97	2.66	0.1252
D	1.33	1	1.33	3.63	0.0775
A*B	0.17	1	0.17	0.48	0.5008
A*C	0.13	1	0.13	0.36	0.5588
A*D	0.15	1	0.15	0.41	0.5347
B*C	1.63	1	1.63	4.46	0.0532
B*D	0.089	1	0.089	0.24	0.6304
C*D	0.38	1	0.38	1.03	0.3271
A*A	1.62	1	1.62	4.43	0.0538
B*B	0.009819	1	0.009819	0.027	0.8722
C*C	0.0004498	1	0.0004498	0.00123	0.9725
D*D	0.41	1	0.41	1.12	0.3070
residual	5.12	14	0.37		
lack-of-fit	4.84	10	0.48	6.94	0.0385
pure error	0.28	4	0.070		
cor total	31.68	28			

2.2.3. Effect of Reaction Temperature. The reaction temperature is ranged from 30 to 90 °C with an interval of 15 °C to investigate the effect of reaction temperature on the adsorption efficiency of vanadium. The other reaction conditions are kept constant: $n(\text{glu})/m(\text{V})$ = 3.0, a reaction time of 60 min, and a H_2SO_4 concentration of 20 g/L. Figure 4 shows that the adsorption efficiency of vanadium increases linearly with the increase of reaction temperature. A low diffusion rate and high viscosity are obtained at low reaction temperature; only 16.81% vanadium is adsorbed at a reaction temperature of 30 °C. A higher reaction temperature can increase the diffusion rate and molecule activity, decrease the viscosity, promote the reaction extent, and enhance the adsorption of vanadium.[45−47] Thus, a reaction temperature of 90 °C is selected for further experiments as a high adsorption efficiency of 91.66% is achieved.

2.2.4. Effect of Reaction Time. The results shown in Figure 5 display the effect of reaction time on the adsorption efficiency of vanadium. The reaction time has a positive effect on adsorption of vanadium, and the adsorption efficiency of vanadium increases with the increasing reaction time. The adsorption efficiency increased rapidly up to 82.28% in the first 20 min, indicating that the adsorption of vanadium is a rapid reaction. With the increasing reaction time, the vacant sites on the surface of GA will reach its saturation, resulting in a lower adsorption rate, and the adsorption efficiency increases slowly: only 7 percentage increase when the reaction time increases from 20 to 40 min and just 0.4 percentage increase from 50 to 60 min. In other words, a further increase in reaction time has no obvious significant effect on the adsorption process; the reaction time can be shortened to some extent.

2.2.5. Response Surface Methodology. The single-factor experiments just investigate the effect of one factor at a time and ignore their interactions on the adsorption process. Thus, the response surface methodology is applied to investigate the interactions and optimize the reaction conditions via Design Expert 8.0 software.[40,47−49] During the analysis process, the single factors are set as independent variables (concentration of H_2SO_4 (A), reaction temperature (B), reaction time (C), and dosage of GA to vanadium ($n(\text{glu})/n(\text{V})$) (D)), and the adsorption efficiency of vanadium is set as the response variable. The actual values for experimental parameters are confirmed according to the single experimental results, which are detailed in Table 1.[40,47−49]

2.2.6. Model Fitting. The experimental results after completing the experiments according to the corresponding experimental conditions are shown in Table 2. The natural log is used to express the simulated results (eq 1):

$$\begin{aligned}\text{Ln}(\eta) = {} & 3.41 - 0.69\text{A} + 1.08\text{B} - 0.28\text{C} + 0.33\text{D} \\ & - 0.21\text{AB} + 0.18\,\text{AC} - 0.19\,\text{AD} + 0.64\,\text{BC} \\ & - 0.15\text{BD} + 0.31\text{CD} - 0.50\text{A}^2 + 0.039\text{B}^2 \\ & - 8.328\text{E} - 003\text{C}^2 - 0.25\text{D}^2 \end{aligned} \quad (1)$$

The coefficients before each parameter represent the direction and influence of the factors on the response (Figure 6). Their coefficients are −0.69, 1.08, −0.28, and 0.33, respectively, which confirms that reaction temperature and dosage of GA show positive impact and that the concentration of H_2SO_4 and reaction time show negative effect on the response, respectively. The order of influence is reaction temperature > dosage of GA > reaction time > concentration of H_2SO_4.

The variance analysis of the polynomial equation is shown in Table 3. The Model *F*-value of 5.19 indicates that the model is significant. The value of "*Prob* > *F*" of 0.0020, which is less than 0.0500, indicates that the model terms are significant and the model can be used to optimize the reaction conditions.

2.2.7. Response Surface Analysis. The contour plots for the effect of the interactions between independent factors on the adsorption efficiency of vanadium are shown in Figure 7. According to the contour plots, the degree of influence of the experimental factors can be judged. As far as the influence of individual experimental factors is concerned, all four factors have great effects on the adsorption efficiency. It is clear that the adsorption efficiency increases with the reaction temperature and dosage of GA and decreases with the concentration of H_2SO_4 and reaction time. The interactions between reaction time and other three factors all have positive effect on the adsorption efficiency, which indicates that long reaction time is

https://doi.org/10.1021/acsomega.1c02590
ACS Omega 2021, 6, 21563−21570

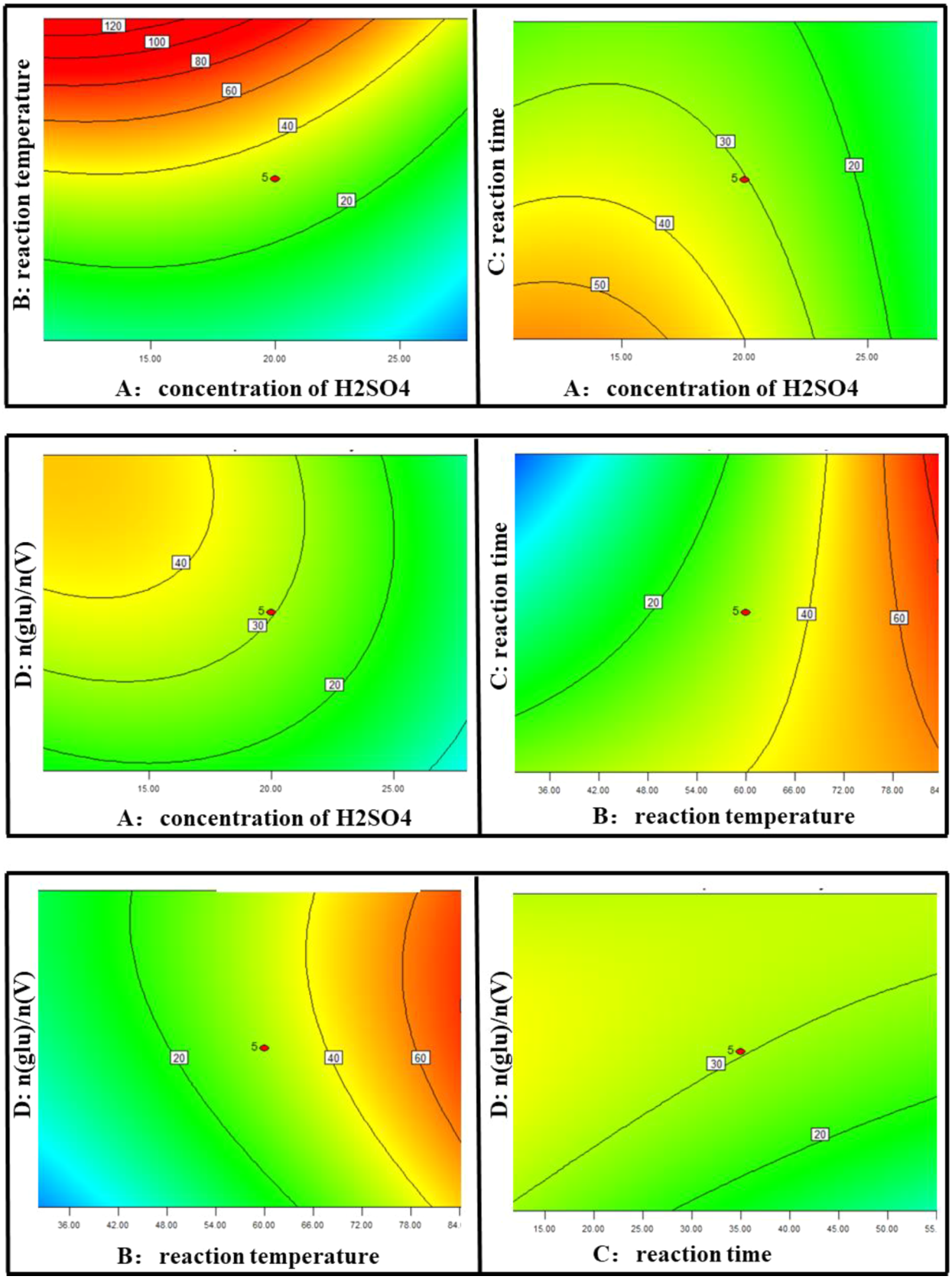

Figure 7. Response surface plots for factors (A to B, A to C, A to D, B to C, B to D, and C to D).

beneficial for the adsorption process, while the interactions between other two factors except reaction time have negative effect on the adsorption process. The results are consistent with the above analysis.

https://doi.org/10.1021/acsomega.1c02590
ACS Omega 2021, 6, 21563−21570

Table 4. Optimization of Reaction Conditions via RSM

optimum conditions				adsorption efficiency/%	
concentration of H2SO4	n(glu)/n(V)	reaction time	reaction temperature	actual	predicted
20 g/L	3.0	35	90 °C	87.25%	86.81%

Table 5. Constants and Correlation Coefficients of Pseudo-Second-Order Kinetic Models for Adsorption of Vanadium with GA (3.0)[a]

temperature	q_e (mg/g)	K	R^2
30	33.30	0.00014	0.9911
45	81.96	0.00017	0.9923
60	108.46	0.00029	0.9978
75	125.34	0.00034	0.9964
90	141.64	0.00108	0.9934

[a] q_e is the adsorption capacity at equilibrium, mg/g; q_t is the adsorption capacity at time t, mg/g. K is the pseudo-second-order sorption model rate constant, g/(mg·min).

Table 6. Thermodynamic Factors of Vanadium Adsorption onto GA (3.0)

temperature	ΔG (kJ/mol)	ΔH (kJ/mol)	ΔS (J/mol K)	R^2
303 K	−0.052	58.50	247.17	0.9718
318 K	−0.066			
333 K	−0.072			
348 K	−0.079			
363 K	−0.085			

2.2.8. Optimization. The optimal reaction conditions are obtained by response surface methodology (RSM), and the results are shown in Table 4. The adsorption efficiency of vanadium is predicted as 86.81% under selected optimum conditions, while the actual adsorption efficiency is 87.25%, which indicates that the selected analysis model is suitable for simulating the adsorption process.

2.3. Kinetic Analysis. In order to better understand the adsorption kinetics of vanadium with GA, the pseudo-second-order kinetic model is selected to analyze the experimental data.[27,28,50] The kinetic model is expressed as eq 2.

$$\frac{t}{q_t} = \frac{1}{Kq_e^2} + \frac{1}{q_e}t \tag{2}$$

The obtained constant coefficients of the kinetic models for vanadium adsorption with GA at different reaction temperatures are shown in Table 5. The adsorption kinetic behavior is significantly affected by the properties of vanadium and GA and reaction conditions. The results displayed in Table 5 showed that the correlation coefficients (R^2) are nearly 1.00, which confirms that the pseudo-second-order model is suitable for describing the adsorption kinetic behavior of vanadium. The q_e and K are calculated with eq 3, and it is observed that the q_e value increased with an increase in reaction temperature, which is consistent with the above analysis that the reaction temperature has the greatest effect on the adsorption efficiency of vanadium. Increasing the reaction temperature can enhance the diffusion rate of vanadium ions to the pores to form new adsorption sites, strengthen the strong bond between vanadium ions and active sites of GA, and increase the chemical interaction between vanadium and GA. Otherwise, the obtained results are in line with some research studies.[27,28]

2.4. Thermodynamic Analysis. The adsorption thermodynamic parameters, including standard Gibbs free energy, standard entropy, and standard enthalpy, are measured to investigate the system energy and matter transformation based on the following equations (eqs 456).

$$\Delta G = -RT\ln K_0 \tag{3}$$

$$\Delta G = \Delta H - T\Delta S \tag{4}$$

$$K_0 = \frac{q_e}{C_e} \tag{5}$$

$$\ln K_0 = \frac{\Delta S}{R} - \frac{\Delta H}{RT} \tag{6}$$

where R is the universal gas constant, 8.314 J/(mol K); T is the reaction temperature, K; K_0 is the equilibrium constant; q_e is the equilibrium concentration of vanadium on the surface of GA, mg/g; C_e is the equilibrium concentration of vanadium in the solution, mg/L.

The thermodynamic analysis is helpful to investigate the reaction mechanism during the adsorption process.[51−53] The calculated results are shown in Table 6. First, the negative value of ΔG displays that the adsorption reaction is feasible thermodynamically and confirms that the adsorption process was physio-sorption (−20 and 0 kJ/mol indicate physio-sorption, −20 to −80 kJ/mol indicates physio-chemi-sorption, and −80 to −400 kJ/mol indicates chemi-sorption). Second, the positive enthalpy (ΔH) indicates that the adsorption process of vanadium with GA was an unspontaneous and exothermic process; meanwhile, it also confirms that the adsorption process is physio-sorption. Finally, the positive entropy (ΔS) value confirms that the adsorption reaction is quite random at the interface of the liquid/solid phase for the vanadium adsorption using GA. Therefore, it is concluded that the adsorption process of vanadium onto GA is an unspontaneous, exothermic, and physio-sorption process.

3. CONCLUSIONS

This paper focused on the adsorption behavior of vanadium with GA. The following conclusions can be obtained:

(1) The optimal processing factors are obtained by RSM, and the influence of processing parameters on the adsorption efficiency of vanadium follows the order reaction temperature > dosage of GA > reaction time > concentration of H_2SO_4. Nearly 91.66% vanadium (adsorption capacity of 101.53 mg/g) can be adsorbed under the optimal conditions: GA dosage at n(glu)/n(V) = 3.0:1, a reaction time of 60 min, a reaction temperature of 90 °C, and a H_2SO_4 concentration of 20 g/L.

(2) The results of the thermodynamic study show that the adsorption process is unspontaneous and exothermic. The values of free energy (ΔG) and standard enthalpy (ΔH) disclose that the mechanism of vanadium adsorption with GA is physio-sorption.

https://doi.org/10.1021/acsomega.1c02590
ACS Omega 2021, 6, 21563−21570

4. MATERIALS AND METHODS

4.1. Materials. All the reagents including sulfuric acid (H_2SO_4), sodium vanadate (Na_3VO_4), and GA ($C_5H_9NO_4$) are of analytical grade, which are purchased from Kelong Co., Ltd., Chengdu, China, and used as received without purification.

4.2. Experimental Procedure. All adsorption experiments are performed in a 300 mL beaker. First, a concentration vanadium solution is added to the beaker, and then, a certain amount of H_2SO_4 is added. The beaker is placed in a water bath. When the solution is heated to a scheduled temperature, GA is added into the solution and then stirred at 500 rpm for the required reaction time.[27,28,43,44] The reaction solution is filtrated by vacuum filtration, and then, the concentration of residual vanadium is determined by inductively coupled plasma−optical emission spectrometry. The adsorption efficiency of vanadium is calculated as follows (eq 7):

$$\eta(\%) = \frac{(C_0 - C_t)}{C_0} \times 100 \quad (7)$$

where C_0 is the initial concentration of vanadium, mg/L; C_t is the concentration of vanadium at different times t, mg/L.

AUTHOR INFORMATION

Corresponding Authors

Hao Peng − *College of Chemistry and Chemical Engineering, Yangtze Normal University, Chongqing 408100, China*; orcid.org/0000-0001-6014-0249; Email: cqupenghao@126.com

Bing Li − *College of Chemistry and Chemical Engineering, Yangtze Normal University, Chongqing 408100, China*; Email: 1127753494@qq.com

Authors

Hongzhi Qiu − *College of Chemistry and Chemical Engineering, Yangtze Normal University, Chongqing 408100, China*

Caiqiong Wang − *College of Chemistry and Chemical Engineering, Yangtze Normal University, Chongqing 408100, China*

Binfang Yuan − *College of Chemistry and Chemical Engineering, Yangtze Normal University, Chongqing 408100, China*

Huisheng Huang − *College of Chemistry and Chemical Engineering, Yangtze Normal University, Chongqing 408100, China*

Complete contact information is available at: https://pubs.acs.org/10.1021/acsomega.1c02590

Notes

The authors declare no competing financial interest.

ACKNOWLEDGMENTS

This work was supported by the Science and Technology Research Program of Chongqing Municipal Education Commission (No. KJQN201901403 and No. CXQT20026) and the Chongqing Science and Technology Commission (No. cstc2018jcyjAX0018).

REFERENCES

(1) Wen, J.; Jiang, T.; Zheng, X.; Wang, J.; Cao, J.; Zhou, M. Efficient separation of chromium and vanadium by calcification roasting−sodium carbonate leaching from high chromium vanadium slag and V2O5 preparation. *Sep. Purif. Technol.* **2020**, *230*, No. 115881.

(2) Rahimi, G.; Rastegar, S. O.; Chianeha, F. R.; Gu, T. Ultrasound-assisted leaching of vanadium from fly ash using lemon juice organic acids. *RSC Adv.* **2020**, *10*, 1685.

(3) Peng, H.; Yang, L.; Chen, Y.; Guo, J.; Li, B. Recovery and Separation of Vanadium and Chromium by Two-Step Alkaline Leaching Enhanced with an Electric Field and H2O2. *ACS Omega* **2020**, *5*, 5340−5345.

(4) Li, H.; Wang, C.; Lin, M.; Guo, Y.; Xie, B. Green one-step roasting method for efficient extraction of vanadium and chromium from vanadium-chromium slag. *Powder Technol.* **2020**, *360*, 503−508.

(5) Gilligan, R.; Nikoloski, A. N. The extraction of vanadium from titanomagnetites and other sources. *Miner. Eng.* **2020**, *146*, No. 106106.

(6) Zhang, W.; Zhang, T.; Lv, G.; Cao, X.; Zhu, H. Thermodynamic study on the V(V)-P(V)-H2O system in acidic leaching solution of vanadium-bearing converter slag. *Sep. Purif. Technol.* **2019**, *218*, 164−172.

(7) Yan, B.; Wang, D.; Wu, L.; Dong, Y. A novel approach for pre-concentrating vanadium from stone coal ore. *Miner. Eng.* **2018**, *125*, 231−238.

(8) Wang, M.; Huang, S.; Chen, B.; Wang, X. A review of processing technologies for vanadium extraction from stone coal. *Miner. Process. Extr. Metall.* **2018**, 1−7.

(9) Liu, C.; Zhang, Y.-M.; Bao, S.-X. Vanadium recovery from stone coal through roasting and flotation. *Trans. Nonferrous Met. Soc. China* **2017**, *27*, 197−203.

(10) Xiao, Y.; Yimin, Z.; Shenxu, B.; Chun, S. Separation and recovery of vanadium from a sulfuric-acid leaching solution of stone coal by solvent extraction using trialkylamine. *Sep. Purif. Technol.* **2016**, *164*, 49−55.

(11) Zhenlei, C.; Yali, F.; Haoran, L.; Yuzhao, Z. Selective Separation and Extraction of Vanadium(IV) and Manganese(II) from Co-leaching Solution of Roasted Stone Coal and Pyrolusite via Solvent Extraction. *Ind. Eng. Chem. Res.* **2013**, *52*, 13768−13776.

(12) Cai, Z.; Feng, Y.; Li, H.; Du, Z.; Liu, X. Co-recovery of manganese from low-grade pyrolusite and vanadium from stone coal using fluidized roasting coupling technology. *Hydrometallurgy* **2013**, *131*−*132*, 40−45.

(13) Li, H.; Fang, H.; Wang, K.; Zhou, W.; Yang, Z.; Yan, X.; Ge, W.; Li, Q.; Xie, B. Asynchronous extraction of vanadium and chromium from vanadium slag by stepwise sodium roasting−water leaching. *Hydrometallurgy* **2015**, *156*, 124−135.

(14) Haixing, F.; Hongyi, L.; Bing, X. Effective Chromium Extraction from Chromium-containing Vanadium Slag by Sodium Roasting and Water Leaching. *ISIJ Int.* **2012**, *52*, 1958−1965.

(15) Deng, R.; Xie, Z.; Liu, Z.; Deng, L.; Tao, C. Enhancement of vanadium extraction at low temperature sodium roasting by electric field and sodium persulfate. *Hydrometallurgy* **2019**, *189*, No. 105110.

(16) Kang, Q.; Zhang, Y.; Bao, S. An environmentally friendly hydrothermal method of vanadium precipitation with the application of oxalic acid. *Hydrometallurgy* **2019**, *185*, 125−132.

(17) Shu, J.; Wu, H.; Chen, M.; Peng, H.; Li, B.; Liu, R.; Liu, Z.; Wang, B.; Huang, T.; Hu, Z. Fractional removal of manganese and ammonia nitrogen from electrolytic metal manganese residue leachate using carbonate and struvite precipitation. *Water Res.* **2019**, *153*, 229−238.

(18) Xiong, P.; Zhang, Y.; Bao, S.; Huang, J. Precipitation of vanadium using ammonium salt in alkaline and acidic media and the effect of sodium and phosphorus. *Hydrometallurgy* **2018**, *180*, 113−120.

(19) Peng, H.; Guo, J.; Li, B.; Liu, Z.; Tao, C. High-efficient recovery of chromium (VI) with lead sulfate. *J. Taiwan Inst. Chem. Eng.* **2018**, *85*, 149−154.

(20) Peng, H.; Guo, J. Removal of chromium from wastewater by membrane filtration, chemical precipitation, ion exchange, adsorption electrocoagulation, electrochemical reduction, electrodialysis, electro-

deionization, photocatalysis and nanotechnology: a review. *Environ. Chem. Lett.* **2020**, 2055.
(21) Zhu, X.; Li, W.; Zhang, Q.; Zhang, C.; Chen, L. Separation characteristics of vanadium from leach liquor of red mud by ion exchange with different resins. *Hydrometallurgy* **2018**, *176*, 42−48.
(22) Bao, S.; Duan, J.; Zhang, Y. Recovery of V(V) from complex vanadium solution using capacitive deionization (CDI) with resin/carbon composite electrode. *Chemosphere* **2018**, *208*, 14−20.
(23) Ye, G.; Hu, Y.; Tong, X.; Lu, L. Extraction of vanadium from direct acid leaching solution of clay vanadium ore using solvent extraction with N235. *Hydrometallurgy* **2018**, *177*, 27−33.
(24) Xiaobo, Z.; Wang, L.; Sen, T.; Majian, Z.; Pengyuan, B.; Lunjian, C. Selective recovery of vanadium and scandium by ion exchange with D201 and solvent extraction using P507 from hydrochloric acid leaching solution of red mud. *Chemosphere* **2017**, *175*, 365−372.
(25) Elwakeel, K. Z.; Guibal, E. Selective removal of Hg(II) from aqueous solution by functionalized magnetic-macromolecular hybrid material. *Chem. Eng. J.* **2015**, *281*, 345−359.
(26) Ming, H.; Bowen, Y.; Chao, S.; Weiming, Z.; Shiya, H.; Lu, L.; Bingcai, P. Simultaneous removal of As(V) and Cr(VI) from water by macroporous anion exchanger supported nanoscale hydrous ferric oxide composite. *Chemosphere* **2017**, *171*, 126−133.
(27) Peng, H.; Liu, Z.; Tao, C. Adsorption Process of Vanadium (V) with Melamine. *Water, Air, Soil Pollut.* **2017**, *228*, 272.
(28) Peng, H.; Liu, Z.; Tao, C. Adsorption kinetics and isotherm of vanadium with melamine. *Water Sci. Technol.* **2017**, *75*, 2316−2321.
(29) El-Sikaily, A.; Nemr, A. E.; Khaled, A.; Abdelwehab, O. Removal of toxic chromium from wastewater using green alga Ulva lactuca and its activated carbon. *J. Hazard. Mater.* **2007**, *148*, 216−228.
(30) Kumar, A.; Jena, H. M. Adsorption of Cr(VI) from aqueous solution by prepared high surface area activated carbon from Fox nutshell by chemical activation with H3PO4. *J. Environ. Chem. Eng.* **2017**, *5*, 2032−2041.
(31) Al-Wakeel, K. Z.; Abd El Monem, H.; Khalil, M. M. H. Removal of divalent manganese from aqueous solution using glycine modified chitosan resin. *J. Environ. Chem. Eng.* **2015**, *3*, 179−186.
(32) Shu, J.; Wu, H.; Liu, R.; Liu, Z.; Li, B.; Chen, M.; Tao, C. Simultaneous stabilization/solidification of Mn(2+) and NH4(+)-N from electrolytic manganese residue using MgO and different phosphate resource. *Ecotoxicol. Environ. Saf.* **2018**, *148*, 220−227.
(33) Szaleniec, M.; Drzewiecka-Matuszek, A.; Witko, M.; Hejduk, P. Ammonium adsorption on Bronsted acidic centers on low-index vanadium pentoxide surfaces. *J. Mol. Model.* **2013**, *19*, 4487−4501.
(34) Miao, Z.; Nihat, H.; McMillan, A. L.; Brusseau, M. L. Transport and Fate of Ammonium and Its Impact on Uranium and Other Trace Elements at a Former Uranium Mill Tailing Site. *Appl. Geochem.* **2013**, *38*, 24.
(35) Zhang, L.; Mu, C.; Zhong, L.; Xue, J.; Zhou, Y.; Han, X. Recycling of Cr (VI) from weak alkaline aqueous media using a chitosan/ triethanolamine/Cu (II) composite adsorbent. *Carbohydr. Polym.* **2019**, *205*, 151−158.
(36) Wang, X.; Lu, J.; Cao, B.; Liu, X.; Lin, Z.; Yang, C.; Wu, R.; Su, X.; Wang, X. Facile synthesis of recycling Fe3O4/graphene adsorbents with potassium humate for Cr(VI) removal. *Colloids Surf., A* **2019**, *560*, 384−392.
(37) Tangtubtim, S.; Saikrasun, S. Adsorption behavior of polyethyleneimine-carbamate linked pineapple leaf fiber for Cr(VI) removal. *Appl. Surf. Sci.* **2019**, *467−468*, 596−607.
(38) Peng, H.; Shang, Q.; Chen, R.; Zhang, L.; Chen, Y.; Guo, J. Step-Adsorption of Vanadium (V) and Chromium (VI) in the Leaching Solution with Melamine. *Sci Rep* **2020**, *10*, 6326.
(39) Peng, H.; Shang, Q.; Cheng, R.; Zhang, L.; Chen, Y.; Guo, J. Highly efficient oxidative-alkaline-leaching process of vanadium-chromium reducing residue and parameters optimization by response surface methodology. *Environ. Technol.* **2020**, 1−10.
(40) Peng, H.; Wang, F.; Li, G.; Guo, J.; Li, B. Highly Efficient Recovery of Vanadium and Chromium: Optimized by Response Surface Methodology. *ACS Omega* **2019**, *4*, 904−910.
(41) Anfar, Z.; Ait Ahsaine, H.; Zbair, M.; Amedlous, A.; Ait El Fakir, A.; Jada, A.; El Alem, N. Recent trends on numerical investigations of response surface methodology for pollutants adsorption onto activated carbon materials: A review. *Crit. Rev. Environ. Sci. Technol.* **2019**, *50*, 1043−1084.
(42) Olmez, T. The optimization of Cr(VI) reduction and removal by electrocoagulation using response surface methodology. *J. Hazard. Mater.* **2009**, *162*, 1371−1378.
(43) Peng, H.; Guo, J.; Wang, B. Adsorption behavior of Fe (III) in aqueous solution on melamine. *Water Sci. Technol.* **2020**, *82*, 1848−1857.
(44) Guo, J.; Chen, R.; Zhang, L.; Shang, Q.; Chen, Y.; Peng, H. Adsorption of Chromium (III) on Melamine: Kinetic, Isotherm Thermodynamics and Mechanism Analysis. *IOP Conf. Ser.: Earth Environ. Sci.* **2020**, *512*, No. 012076.
(45) Peng, H.; Yang, L.; Chen, Y.; Guo, J.; Li, B. Recovery and Separation of Vanadium and Chromium by Two-Step Alkaline Leaching Enhanced with Electric Field and H2O2. *ACS Omega* **2020**, *5*, 5340−5345.
(46) Peng, H.; Leng, Y.; Guo, J. Electrochemical Removal of Chromium (VI) from Wastewater. *Appl. Sci.* **2019**, *9*, 1156.
(47) Peng, H.; Leng, Y.; Cheng, Q.; Shang, Q.; Shu, J.; Guo, J. Efficient Removal of Hexavalent Chromium from Wastewater with Electro-Reduction. *Processes* **2019**, *7*, 41.
(48) Peng, H.; Shang, Q.; Chen, R.; Leng, Y.; Guo, J.; Liu, Z.; Tao, C. Oxidative Leaching Kinetics of Vanadium from the Vanadium-Chromium-Reducing Residue with K2Cr2O7. *ACS Omega* **2020**, *5*, 8777−8783.
(49) Zhang, X.; Liu, Z.; Fan, X.; Lian, X.; Tao, C. Optimization of reaction conditions for the electroleaching of manganese from low-grade pyrolusite. *Int. J. Miner., Metall. Mater.* **2015**, *22*, 1121−1130.
(50) Ho, Y. S.; McKay, G. Pseudo-second order model for sorption processes. *Process Biochem.* **1999**, *34*, 451−465.
(51) Wu, C. H. Adsorption of reactive dye onto carbon nanotubes: Equilibrium, kinetics and thermodynamics. *J. Hazard. Mater.* **2007**, *144*, 93−100.
(52) Afroze, S.; Sen, T. K.; Ang, M.; Nishioka, H. Adsorption of methylene blue dye from aqueous solution by novel biomass Eucalyptus sheathiana bark: equilibrium, kinetics, thermodynamics and mechanism. *Desalin. Water Treat.* **2016**, *57*, 5858−5878.
(53) Konggidinata, M. I.; Chao, B.; Lian, Q.; Subramaniam, R.; Zappi, M.; Gang, D. D. Equilibrium, kinetic and thermodynamic studies for adsorption of BTEX onto Ordered Mesoporous Carbon (OMC). *J. Hazard. Mater.* **2017**, *336*, 249−259.

https://doi.org/10.1021/acsomega.1c02590
ACS Omega 2021, 6, 21563−21570